Title: Modelling of structure and properties of pearlitic steel and abrasive wear of the turnout frog in the cyclic loading conditions

Author: Jerzy Herian, Krzysztof Aniołek.

Citation style: Herian Jerzy, Aniołek Krzysztof. (2011). Modelling of structure and properties of pearlitic steel and abrasive wear of the turnout frog in the cyclic loading conditions. "Journal of Achievements in Materials and Manufacturing Engineering" (Vol. 49, iss. 1 (2011), s. 71-81).

Journal of Achievements in Materials and Manufacturing Engineering
VOLUME 49
ISSUE 1
November
2011

Modelling of structure and properties of pearlitic steel and abrasive wear of the turnout frog in the cyclic loading conditions

J. Herian [a,*], K. Aniołek [b]
[a] Department of Materials Technology, Silesian University of Technology, ul. Krasińskiego 8, 40-019 Katowice, Poland
[b] Institute of Materials Science, University of Silesia, ul. Bankowa 12, 40-007 Katowice, Poland
* Corresponding author: E-mail address: jerzy.herian@polsl.pl

Received 11.09.2011; published in revised form 01.11.2011

Analysis and modelling

ABSTRACT

Purpose: Analysis of pearlite morphology changes as a result of hot rolling process and isothermal annealing.
Design/methodology/approach: Physical modelling of isothermal annealing for a transition point of 520-620°C was carried out using a Gleeble simulator. A scanning electron microscope was used for a quantitative evaluation of the microstructure. In numerical estimations there were marked distributions of the loads and then distributions of the contact stresses and the strains in places of contact wheel-switch components. Tests of resistance to abrasive wear were carried out at the Amsler stand.
Findings: The obtained test results confirm that these methods can be effectively used in shaping the pearlitic structure and properties of the steel.
Practical implications: In physical modelling of tests of resistance to abrasive wear for the steel grade R260 after hot rolling and isothermal annealing it has been proved that this feature is a function of the steel structure and properties in the given operation conditions. The resistance to abrasive wear of steel R260 with a pearlitic structure and different pearlite morphology decreases with the increase of load and slide. From conducted numerical calculations result that the biggest dynamic load is in the moment of a drive of a wheel set on a frog of the turnout. The value of the vertical force depends on speed and mass of the railway vehicle.
Originality/value: An advantageous pearlitic morphology of steel (block sections) with interlamellar distance in the order of 0.12-0.13 μm, ensuring hardness of about 340-350 HB, is facilitated by a hot rolling process combined with isothermal annealing.
Keywords: Pearlite morphology; Abrasive wear; Railroad switches; Block sections; Load; Contact stresses; Numerical modeling

Reference to this paper should be given in the following way:
J. Herian, K. Aniołek, Modelling of structure and properties of pearlitic steel and abrasive wear of the turnout frog in the cyclic loading conditions, Journal of Achievements in Materials and Manufacturing Engineering 49/1 (2011) 71-81.

1. Introduction

Railway turnouts either fork or join intersecting tracks (Figs. 1, 2). For this reason, they constitute important elements of the track infrastructure in railway lines. When rail vehicles ride over, components of turnouts are especially exposed to abrasive and fatigue wear, including changes of the rolling surface shape in consequence of dynamic loads of a cyclic nature. Life of railway turnouts depends on the functional properties of the material they are made from and on the operating conditions.

Sections composing rail tracks and switches (Fig. 3, Table 1) must meet high requirements in the scope of the material properties, its shape and continuity [1, 2].

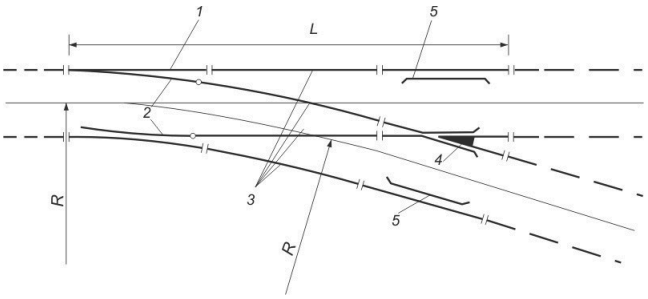

Fig. 1. Ordinary railroad switch: 1 – stock rail, 2 – blade, 3 – connecting rails, 4 – frog, 5 – guard rail, L – length, R – radius

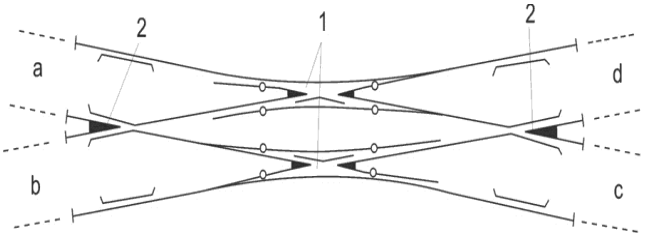

Fig. 2. Scissors crossover : 1 – double frogs, 2 – single frogs

Block sections of KL49 and KL69 type produced with the use of hot rolling method are widely applied in the construction of ordinary and scissors railway switches. The measurements of block sections wear in operational conditions, built in the frog switches have identified certain irregularities in the rolling surface profile wear of the actual frog point (Fig. 4) and its plastic flattening. The biggest wear occurs on the actual frog point in the place of the biggest load, which decreases as the distance from the frog point increases. Such wear is caused by the momentary increase of the dynamic load acting on a small rolling surface of the frog point. It leads to the intensive wear and flattening as a result of the rail vehicle wheel hits. For the reasons mentioned above, materials used for the production of sections in the rail switches must have specific properties and first of all an increased resistance to abrasive wear and fatigue [1-6, 12, 13, 16, 17]. High costs of rail switches operation and their exchange are the grounds for the preparation of new materials or technologies for the production of sections of wear increased in relation to the ones currently used.

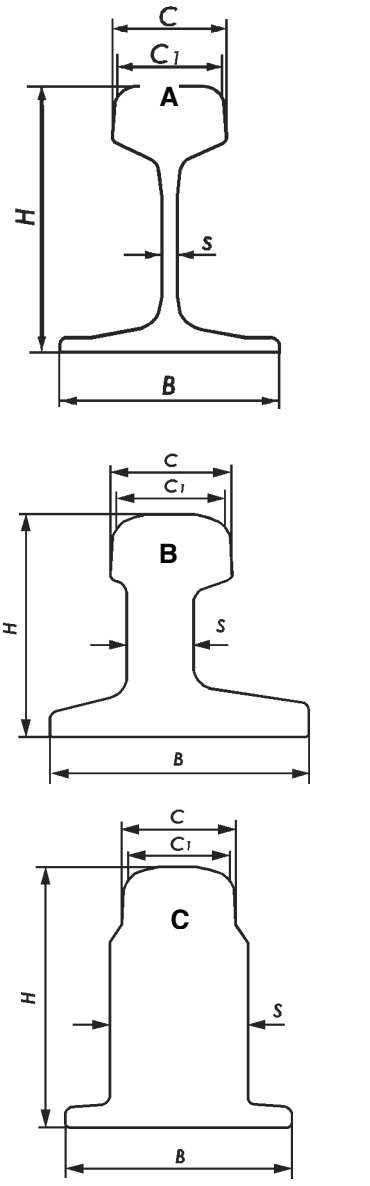

Fig. 3. Sections: a - rail, b- needle, c- block

Table 1.
Dimensions of rail sections

Type	Dimensions, mm				
	H	C	C_1	B	s
60E1 (rail)	172	-	72	150	16.5
I60 (needle)	139	72	70.6	160	40
KL60 (block)	172	74.3	72	150	90

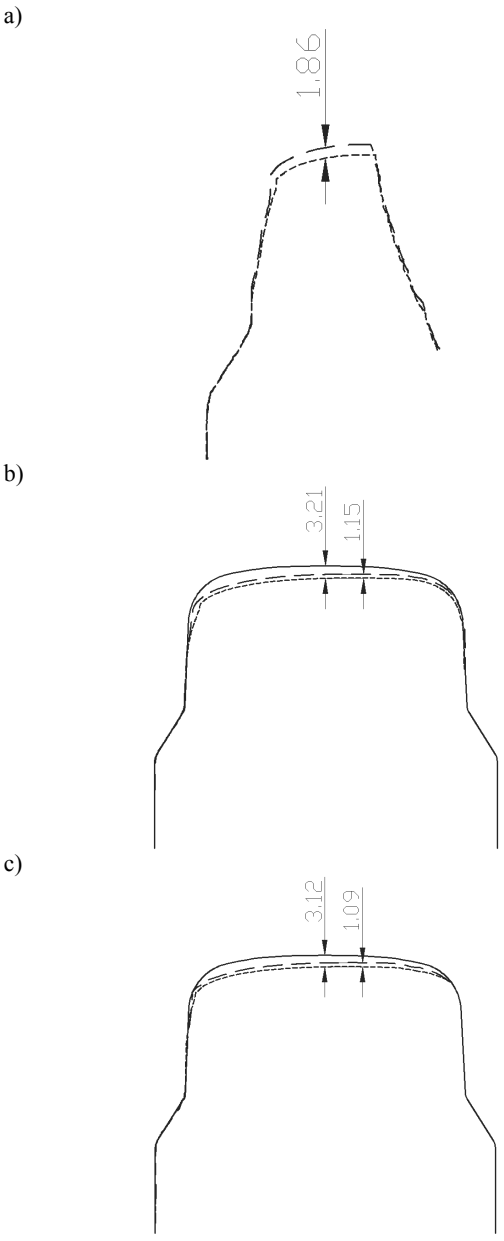

Fig. 4. Vertical wear on the cross-section of the KL60 section in the distance from the actual frog point: a – 10 cm, b – 60 cm, c – 110 cm

A basic grade of steel used for the production of rails and sections for railroad switches is carbon-manganese steel with a pearlitic structure. The European Rail Standard (PN-EN 13674) distinguishes seven pearlitic steel grades, the hardness of which varies in a wide range from 200 to 390 HB. The most commonly applied grade of rail steel is R260, which is not only used for the production of rails but also for the production of needle and block sections. This grade of steel is characterised by high levels of endurance and hardness, good resistance to abrasive wear, as well as lower ductility and crack resistance.

High levels of pearlitic steel resistance and hardness at sufficient ductility level may be obtained thanks to the application of appropriate production techniques, controlled rolling and heat treatment – isothermal annealing. The strengthening of the material in the process of rolling may be regulated by means of the deformation parameters and the temperature at the end of rolling or, in the process of isothermal annealing, by means of the initial austenite grain size, transition temperature and rate of cooling from the austenitizing temperature to the isothermal holding temperature, until total disintegration of austenite. The controlled rolling or heat treatment results in size reduction of pearlite colonies and in reduction of the interlamellar distance in cementite. Changing the morphology of the pearlite allows for the regulation, within a wide range, of the steel properties and the durability of rail sections [1, 2, 7-11].

A component that is particularly exposed to the action of high dynamic loads is the frog applied in the place where stretches of rails of the principal and diverging tracks intersect. Discontinuity in a stretch of rails leads to high dynamic loads caused by vehicle wheels striking against the frog point. The impact load grows in specific operating conditions as the turnout frog wear increases as a result of lowering of the frog point height in relation to the switch rails. In the place of the frog's contact with the wheel, a particular state of contact stress is present, induced by the load coming from the rail vehicle [18, 19]. Highest contact stresses often reach values which exceed numerically the yield point and the tensile strength limit of the material. In the immediate neighbourhood of the contact area, these stresses may achieve values which will lead to plastic deformation followed by loss of cohesion in the material. This is manifested by accelerated destruction of the material from which the rail sections are made. Subsurface cracks are formed which, while propagating, lead to material failure. The load present in the wheel/rail contact point determines the operating conditions and durability of the turnout. The forecasting of the distribution of stresses induced by operational loads on the wheel-frog point contact surface will enable determining the places particularly exposed to loss of material continuity. Such knowledge should form the basis for the correct design of the architecture of turnouts and for choosing the material for their components.

2. Research material

Block sections of KL60 type, hot-rolled, made of rail steel of R260 grade have been chosen for the purposes of the research. The rolling of sections of ingots coming from continuous casting has been conducted in a line unit. The temperature at the end of rolling was about 930°C. Cooling was performed in a refrigeration plant in smooth air. The control analysis of the chemical composition of steel has been performed using an ARL 3460 multichannel emission spectrometer. The chemical composition and mechanical properties of steel after hot rolling are presented in Table 2.

Friction couples made of materials used in interacting elements in real conditions were used in the abrasive wear resistance tests at the Amsler stand. P60 steel (C – 0.63%, Mn – 0.82%, Si – 0.27%, Cr – 0.02%) was used as a counter-specimen. This type of steel is commonly used in rail wheel rings.

Table 2.
Chemical composition and properties of R260 steel

Steel grade	Content of chemical elements, %							
	C	Mn	Si	P	S	Cr	Al	V
R260	0.74	1.08	0.31	0.013	0.018	0.040	0.003	0.004
	Mechanical properties							
	UTS, MPa		YP, MPa		Elongation, %		pct RE, %	
	923		528		11.4		15.9	

3. Research methodology

3.1. Heat treatment

The pearlitic structure of R260 steel with a varied pearlite morphology was obtained during physical modelling of isothermal annealing on a Gleeble 3800 simulator in the Institute for Ferrous Metallurgy (Instytut Metalurgii Żelaza) in Gliwice. This simulator ensures maintaining high measurement accuracy and austenitization temperature control, a constant temperature of pearlitic transition in time and a constant cooling rate. Ring-shaped specimens with the dimensions of ϕ32x10 mm made of KL60 block section (Fig. 5) were used in modelling of the isothermal annealing process.

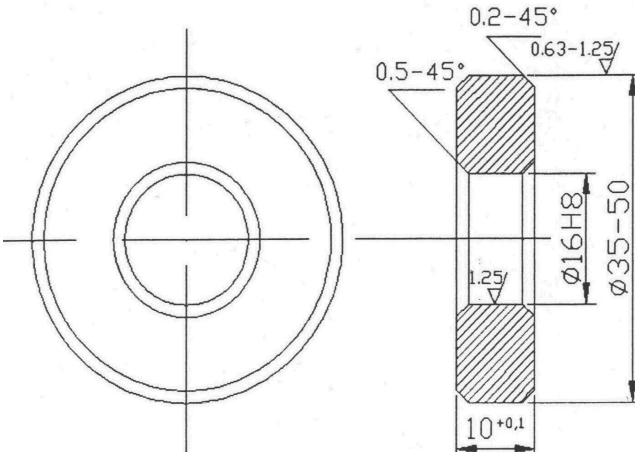

Fig. 5. Specimens for abrasive wear tests at the Amsler stand

The parameters of heat treatment of steel were determined on the basis of dilatometric tests and the results of structural tests of steel after isothermal annealing. The parameters of the heat treatment on the Gleeble simulator were as follows:

- heating of the specimens up to austenization temperature of 800°C,
- annealing in the temperature of 800°C for 720 s,
- cooling of the specimens at a rate of 15°C/s to the isothermal holding temperature (620, 570, 550 and 520°C),
- isothermal holding for 300s and cooling the specimens to ambient temperature at a rate of 15°C/s.

3.2. Microstructure tests

Microstructure tests were performed with the application of a HITACHI S-3400N scanning electron microscope on specimens that have undergone the process of hot rolling and isothermal annealing. Specimens for the observation of the microstructure were taken from rings used to test the abrasive wear resistance. In order to reveal the pearlite colonies, the specimens, after hot rolling, were etched with 3.5% nital, and after annealing, with an isothermal solution of picric acid. During the observation and measurement of the interlamellar distance, magnifications of 2000 up to 15000x were used.

3.3. Quantitative description of the pearlitic structure

The measurements of interlamellar distance in cementite in R260 steel in the state after hot rolling and isothermal annealing were performed on a HITACHI S-3400N scanning electron microscope at a magnification of 15000x. 32 pearlite colonies were analyzed for the variant from the state after hot rolling, as well as for each variant after isothermal annealing. In each colony, the number of intersections with cementite lamellae was counted along a section perpendicular to cementite lamellae. During the measurements, various lengths of the section were used, depending on the arrangement of the lamellae and size of a given pearlite colony. The applied measurement methodology is a new one which differs from the methodologies applied so far. The distance between the lamellae, µm, was calculated according to the following dependence:

$$l = \frac{a}{n}$$

where: a – length of the section perpendicular to the cementite lamellae, µm; n – number of intersections of the section with the cementite lamellae.

3.4. Determination of hardness and tensile strength

For the purpose of determining those properties, measurements of hardness were performed, as well as a static tensile test on cylindrical specimens of a special shape. Measurements of the material hardness after hot rolling and isothermal annealing were performed on a KP15002P hardness tester, with the application of the Brinell method, using a ball with a 2.5 mm diameter and a load of 1839N.

Tensile strength of steel with a pearlitic structure and with different morphologies was determined in a static tensile test on specimens with neck in the central part (Fig. 6).

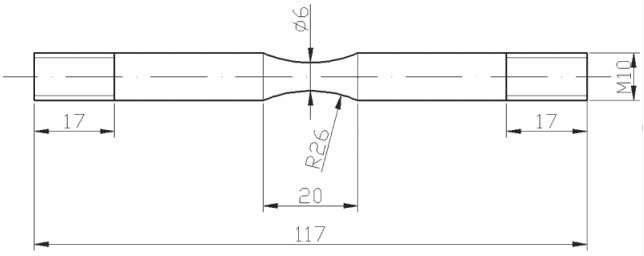

Fig. 6. Dimensions of specimens for strength tests after heat treatment

3.5. Modelling the load of railway turnout in the Universal Mechanism program

In the numerical modelling of the dynamics of the rail vehicle-track system, programs such as VI Grade Adams/Rail or Universal Mechanism are used. The Universal Mechanism program was used for modelling the dynamic phenomena present during a rail vehicle travelling through a turnout [14, 15]. An ordinary right turnout was modelled (Fig. 1) with the diverging tract radius of 300 m and frog angle of 1:9. The turnout model was built based on the results of measurements of the cross-section profile of the switch and frog (Fig. 7). For that purpose, a Graw X-Y laser profilometer was used. Measuring points were selected so as to reflect the change of profiles in a real turnout. The obtained cross-section contours were adjusted to the form required in the Universal Mechanism program. Next, the consecutive cross-sections were put together in accordance with the profiles measured in the real turnout. The adopted length of the investigated track section was 200 m. The turnout switch had its beginning at 100 m and the frog, at 128 m of the turnout. Before and after the turnout, there was a straight section of track with rails of type UIC 60.

A built mathematical models of the turnout and Diesel locomotive SM42 were used in the modelling process. They were next subjected to a dynamic analysis. Simulation for the principal track and ordinary turnout was conducted at rail vehicle speeds of 20 and 80 km/h. The values of vertical forces (F_z) and transverse forces (F_y) were determined as functions of time and distance. The results obtained in the simulation are presented in Fig. 12 and Table 4.

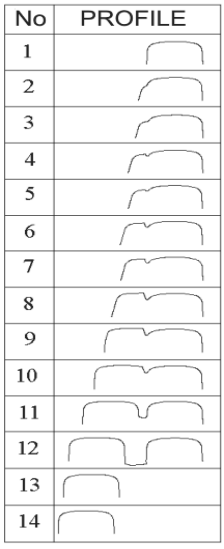

Fig. 7. Change of the cross-section profiles throughout the turnout length

3.6. The modelling of the distribution of stresses and deformation at the wheel/block section contact surface

The modelling of the wheel-block section contact interaction is a difficult task due to the complex shape of the rolling profile of the wheel and the section. The MSC MARC computer application based on the finite element method (FEM) was used in the numerical analysis of stress distribution. The application allows non-linear determination of contact and reduced stresses, as well as plastic deformations [18].

The building of a model for the calculation of stresses and deformation consisted of three stages. In the first stage, a flat model of cross-sections of the wheel and the block section was created in the "wxProfile" application and the contact point was determined. A centred position was adopted for modelling, which means that the centre of the cross-section of the block section was aligned with the pitch diameter of the wheel. The flat model prepared in the "wxProfile" application was then exported to the MSC.visualNastran application for Windows. The latter application was used to create a spatial model out of the flat one. It was assumed in the calculations that the wheel material was steel P60, which is used in rail wheel rings, and the KL60 block section material was the R260 steel, both with plastic-elastic characteristics. Essential values, such as Young's modulus (E) and Poisson's coefficient (ν) for the material of the block section and of the rail vehicle wheel were determined in experimental tests. For steel P60 the values equalled: $E=2.06\cdot10^5$ MPa and $\nu=0.27$, and for R260, $E=2.10\cdot10^5$ MPa and $\nu=0.25$.

In the next stage, discretization of the model was performed, i.e. a division into finite elements (the so-called mesh). Thus prepared model was exported from MSC.visualNastran for Windows to the MSC.MARC application. Due to the complexity of the model (a large number of finite elements), only a part of the

block section and a fragment of the wheel ring were modelled. An area of compact mesh was created in the spot where the contact was expected to occur, in order to gain more precise results.

Suitable constraints were prescribed in the MSC MARC application by fastening upper wheel nodes in directions X, Y and Z and block section nodes in the X direction. For technical reasons, the model of the wheel was immobilized and the block section was weighed down at its lower area with a force directed towards the rolling surface. It was assumed in the analysis that the wheel diameter corresponded to the SM42 locomotive (1100 mm) and that the load values were varied. The values of vertical forces determined in the Universal Mechanism application were used to prescribe correct boundary conditions in the MSC MARC application. Next, the so prepared model was subjected to numerical calculations. The calculations were performed for various load values of the KL60 block section. The distributions of stress and deformation are presented in Figs. 13-15.

3.7. Tests of resistance to abrasive wear in the conditions of rolling-sliding friction

Tests of resistance to abrasive wear were carried out at the Amsler stand with a tribological pair of a roller-roller type. The materials tested, in the form of rings, were fastened on two shafts moving in opposite directions. The skid value between the specimen and the counter-specimen was regulated by changing the diameter of the counter-specimen. The load was regulated by means of a spring mechanism. Two load values were assumed (663 and 903 MPa) and a skid value of 1%. The tests were carried out in a range up to 54,000 cycles in 18 research stages. The applied test parameters corresponded to real operating conditions of railroad switches.

Tribological tests were performed with the application of friction couples interacting in real conditions. The material for the specimens was R260 steel with a diverse pearlite morphology.P60 steel was used as a counter-specimen. This type of steel is commonly used in rail wheel rings so its application increased the credibility of R260 steel wear results.

4. Tests results

4.1. Steel microstructure after hot rolling and isothermal annealing

The identification of the microstructure of the examined steel was performed using a scanning electron microscope. It has been found that in the steel after hot rolling there is a pearlitic microstructure, formed by pearlite colonies of various arrangement directions (Fig. 8).

The material after isothermal annealing demonstrated a pearlitic structure with finer colonies in relation to the colonies after hot rolling. The microstructures after heat treatment were characterized by a smaller interlamellar distance and smaller thickness of cementite lamellae (Fig. 9). On the boundaries of former austenite grains ferrite bands were observed.

a)

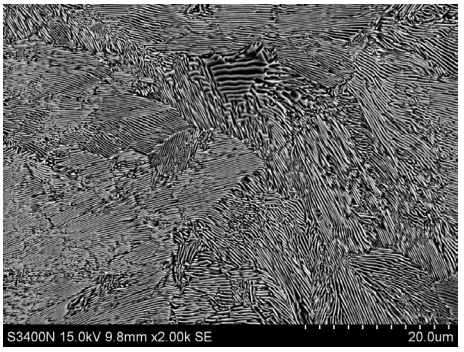

b)

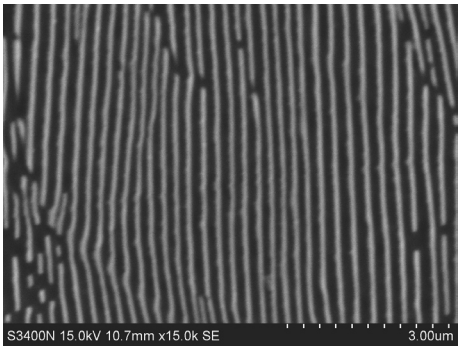

Fig. 8. The microstructure of steel in the state after hot rolling

a)

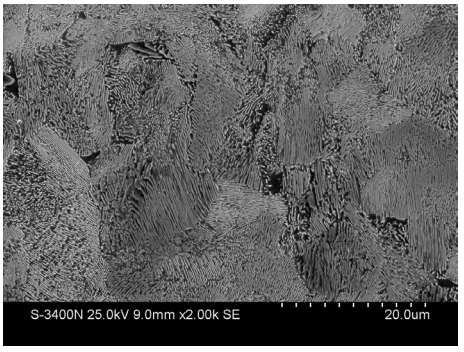

b)

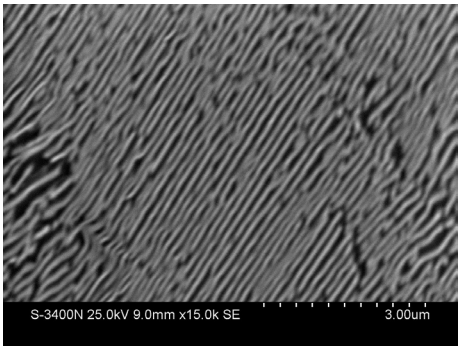

Fig. 9. The microstructure of steel R260 after isothermal annealing at the temperature 620°C

4.2. Quantitative description of the microstructure of pearlitic steel

The measurement results of an interlamellar distance and hardness are demonstrated in Table 3. Depending on adopted parameters for heat treatment, the material contained a pearlitic microstructure with various interlamellar distances in cementite. The steel after hot rolling contained an average interlamellar distance of 0.28 μm while after isothermal annealing from 0.12 to 0.17 μm (Table 3). The lowering of an isothermal holding temperature caused the reduction of an interlamellar distance. The smallest average cementite interlamellar distance of 0.12 μm was obtained in case of the material annealed isothermally at the temperature of 520°C.The interlamellar distance reduced in this case more than two times in relation to the state after hot rolling.

Table 3.
An interlamellar distance in pearlite colonies

	Interlamellar distance of l_t, μm			Standard deviation	Hardness HB
	minimum	maximum	average		
As-rolled condition	0.18	0.35	0.28	0.05	274
OC 620°C	0.14	0.26	0.17	0.02	301
OC 570°C	0.11	0.20	0.14	0.02	325
OC 550°C	0.11	0.17	0.13	0.01	338
OC 520°C	0.10	0.15	0.12	0.01	350

4.3. Mechanical properties

The average results of five hardness measurements depending on an interlamellar distance in cementite are shown in table 3 and Fig. 10. The reduction of an interlamellar distance results in the increase of material hardness, which is in accordance with the data included in the references. The material after hot rolling is characterized by considerably lower hardness in comparison with the material after isothermal annealing. It is caused by pearlite morphology, a size reduction of colonies and the reduction of an interlamellar distance.

The lowering of an annealing temperature results in the increase of tensile strength. This increase of tensile strength is caused by a smaller interlamellar distance in cementite (Fig. 11) and smaller thickness of cementite lamellae.

The comparison of tensile strength for two examined different material states has shown that the material after isothermal annealing was characterized by the tensile strength of 300 to 400 MPa higher in comparison with the material after hot rolling. This fact is reflected by a similar pattern of a thickness change. The increase of strength properties resulting from the reduction of an interlamellar distance caused the change of steel resistance to abrasive wear, which has been proven in own examinations.

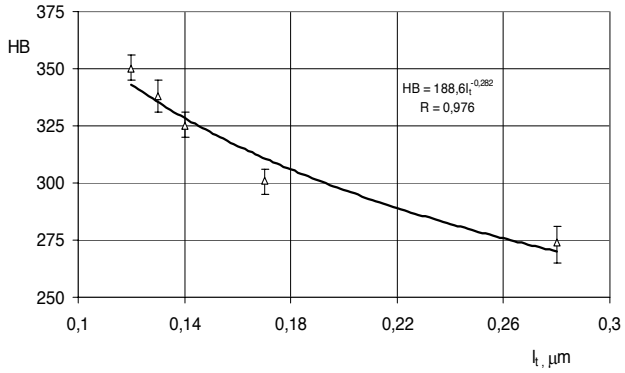

Fig. 10. The changes of HB hardness depending on an interlamellar distance l_t

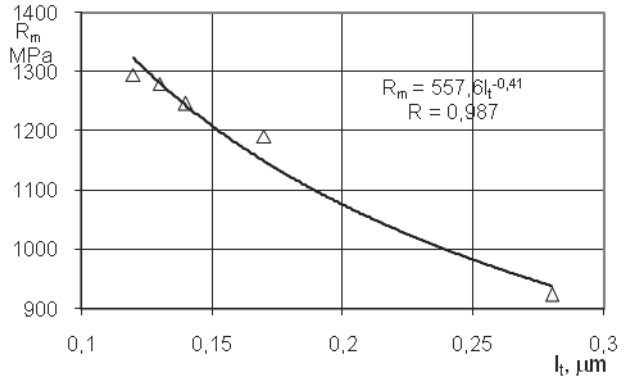

Fig. 11. The influence of an interlamellar distance l_t on steel tensile strength

4.4. Modelling the load of railway turnout

The load distribution during the rail-vehicle ride through the turnout is of a dynamic nature. The obtained results of numerical forecasting of the load corroborate the presence of high values of load acting on the turnout components and in particular, on the frog. Railway turnout frogs are exposed to the action of a variable force which occurs in two planes: vertical and horizontal. The value of the vertical force depends on the speed and mass of the rail vehicle (Fig. 12).

On a straight track section before the turnout, the vertical force was constant and amounted to about 92.5 kN. Dynamic load appeared at the moment the wheel set ran onto the turnout points. During the transfer of the load from the stock rail to the switch blade (the right rail), a small decrease in the vertical force was observed, followed by its increase and next, the vertical force amplitude stabilized until the wheel ran onto the frog.

The biggest dynamic loads appear at the moment the wheel set runs onto the frog. The impact of the wheel against the actual frog point is visible as a high peak in the diagram of the vertical and shearing forces over time (Fig. 12). During the further ride of the wheel set through the actual frog point, the dynamic load

decreases, after which the vertical force amplitude falls down and gradually stabilizes. This force will reach 119 kN in the principal track of the turnout at a speed of 20 km/h, due to the lack of rail continuity in the frog section. The vertical force value increases to 188 kN as the speed increases to 80 km/h. Essentially, the vehicle speed does not have any effect on the value of shearing force. Before the turnout, this value was close to zero and at the moment of striking against the frog point, it was between 32 and 34 kN.

Table 4.
Values of the maximum vertical and transverse forces present at the frog of an ordinary turnout

Direction	Speed, km/h	Vertical force Fz, kN	Transverse force Fy, kN
Main track	20	117	32.7
Main track	40	153	34.3
Main track	60	172	33.1
Main track	80	188	32.4

4.5. The modelling of the distribution of stresses and deformation

During the interaction of the wheel (28UI140) with the block section (KL60), the stresses concentrate in the outermost area of the rolling surface of the block section. Stress values depend strictly on the load present in the wheel – block section couple. The biggest reduced stresses occur in the contact zone and under the rolling surface of the block section. At a load of 153 kN, the maximum reduced stresses amount to 617 MPa and at a load of 188 kN, they reach 667 MPa (Figs. 13, 14). The determined reduced stresses exceed the yield point value ($R_{p0.2}$=528 MPa), which results in the flattening of the rolli ng surface of the turnout frog point component (the block section). The flattening was observed and confirmed in operational tests of the wear of railway turnout frogs. The flattening may initiate microcracking on the rolling surface, the consequence of which may be damage caused by material failure.

An increase of load also effects the value and distribution of contact stresses. With a dynamic load of 188 kN, the contact stresses are higher by almost 500 MPa and the zone of their effect slightly grows (Figs. 13, 14). Similarly is in the case of plastic deformations which also depend on the load present in the wheel – block section system. The zone of occurrence of plastic deformation grows as the load increases (Fig. 15). The results obtained are corroborated by real data which show that frog points are subject to accelerated abrasive and contact failure wear. The forecasting of the distribution of load and of the future contact stresses and deformation allows the rational design of railway turnouts and is useful for a correct selection of material to be used for their components.

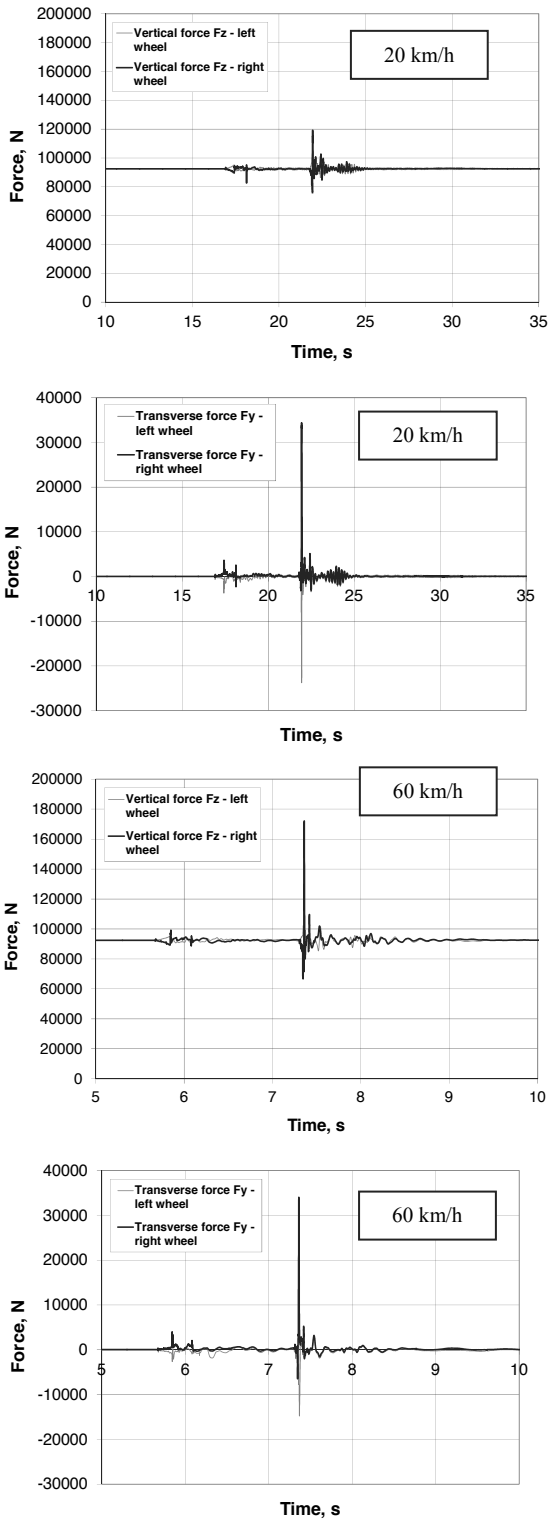

Fig. 12. Marked distributions of vertical strength for different speeds of the railway vehicle ride through a basic track of an ordinary railroad switch

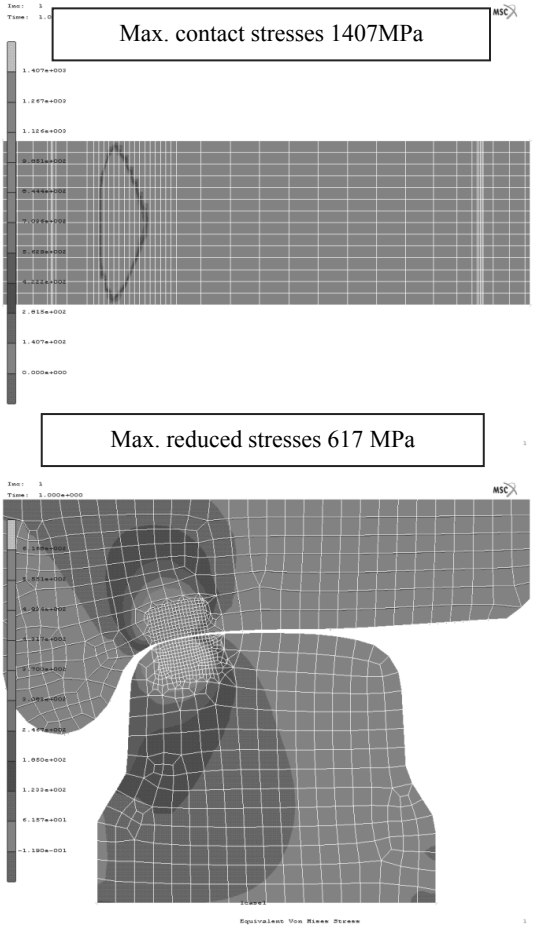

Fig. 13. Distribution of standard contact stresses (a) and supplementary (b) for a block section KL60 with the load of 153 kN appointed in the Universal Mechanism program

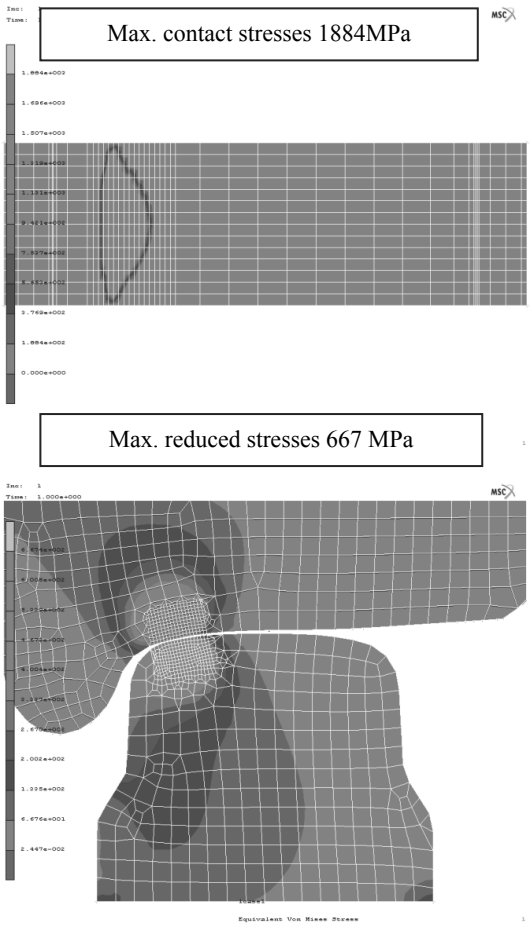

Fig. 14. Distribution of standard contact stresses (a) and supplementary (b) for a block section KL60 with the load of 188 kN appointed in the Universal Mechanism program

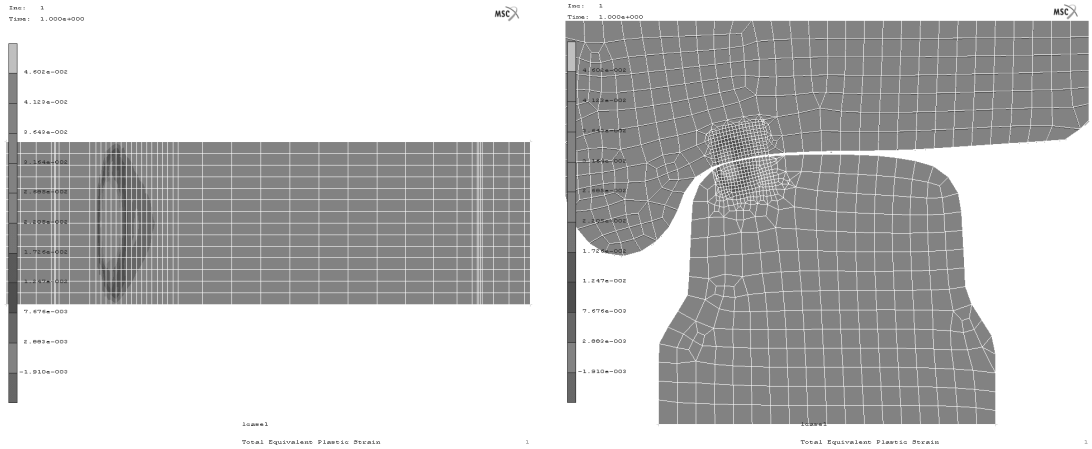

Fig. 15. Distribution of plastic strains for the block section KL60 with the load of 188 kN appointed in the Universal Mechanism program

4.6. Tests of resistance to abrasive wear

In the tests of the resistance to abrasive wear in the conditions of rolling-sliding friction of steel with different pearlite morphology, it has been demonstrated that material wear is dependent on operational parameters and an interlamellar distance in cementite. No abrasive wear was observed in the number of cycles ranging from 8000 to 12000. Above 12000 cycles, the wear assumes the characteristics similar to linear (Figs. 16-19). The steel after hot-rolling (l_t=0.28 μm) was characterized by the lowest resistance to abrasive wear, demonstrating the highest wear for the tested values of pressure. The abrasive wear of rail steel is the more intensive, the larger load at a constant slide is. The material after isothermal annealing characterized by a smaller interlamellar distance in cementite underwent lower abrasive wear, proving that resistance to abrasive wear increases with the decrease of an interlamellar distance in cementite of pearlitic structure. For instance, the wear of hot rolled material of l_t=0.28 μm was 1.25 times higher than the abrasive wear of material of l_t=0.12 μm after annealing at the temperature of 520°C (Fig. 13). Thus, the use of block sections made of steel with pearlitic structure and a small interlamellar distance on switch elements will significantly increase resistance to abrasive wear and, at the same time, prolong their operational period.

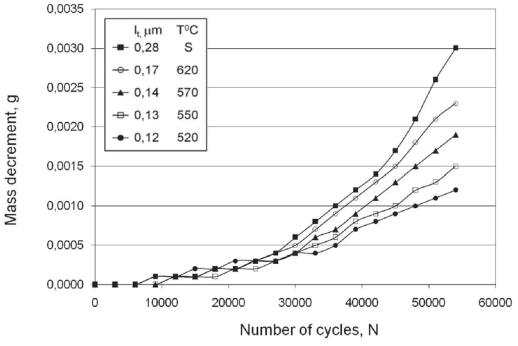

Fig. 16. The course of the abrasive wear of steel R260 with a different interlamellar distance in cementite depending on a number of cycles for the slide of γ=0.1% and the pressure of 663MPa using steel P60 as a counter specimen

5. Conclusions

The increase of rail vehicles speed, load and pressure as well as the frequency of travelling must be accompanied with such a selection of materials which will ensure lower wear of rail sections and prolong the durability period of turnouts and railroads. A method which leads to increasing the resistance to abrasive wear of high-carbon steel with a pearlitic structure is the modification of its morphology. The morphology of pearlite may be controlled to a large degree by means of isothermal annealing parameters. The properties of the material from which rail sections are manufactured can be controlled by changing the size of pearlite colonies and an interlamellar distance in cementite.

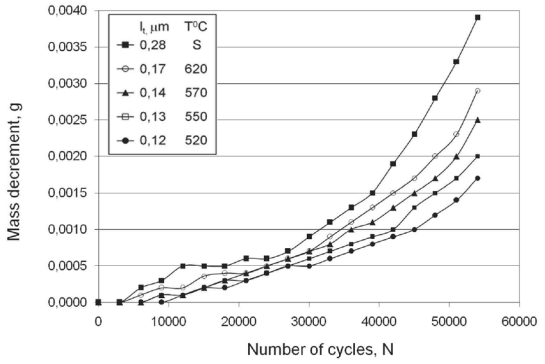

Fig. 17. The course of the abrasive wear of steel R260 with a different interlamellar distance in cementite depending on a number of cycles for the slide of γ=0.1% and the pressure of 903 MPa using steel P60 as a counter specimen

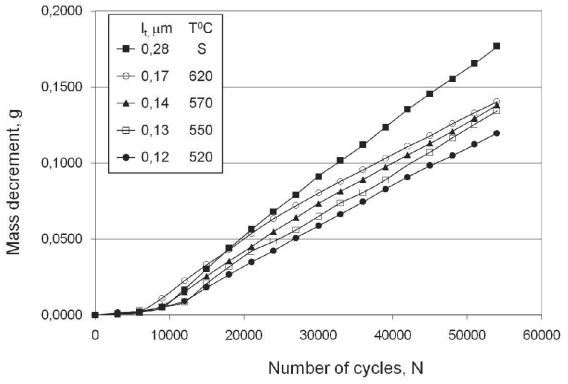

Fig. 18. The course of the abrasive wear of steel R260 with a different interlamellar distance in cementite depending on a number of cycles for the slide of γ=1% and the pressure of 663 MPa using steel P60 as a counter specimen

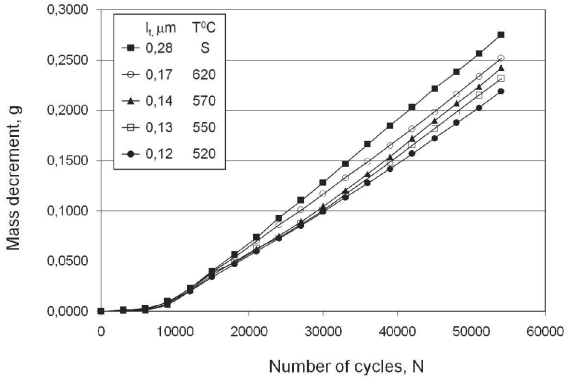

Fig. 19. The course of the abrasive wear of steel R260 with a different interlamellar distance in cementite depending on a number of cycles for the slide of γ=1% and the pressure of 903 MPa using steel P60 as a counter specimen

On the basis of tests made, it was found that the microstructure of steel R260 after isothermal annealing at the temperature range of 520-620°C contained reduced in size pearlite colonies, a more than two times smaller interlamellar distance in cementite (l_i=0.12-0.17 μm) than the distance in the steel after hot rolling (l_i=0.28 μm). A reduction of annealing temperature results in a reduction of the interlamellar distance and an increase of steel hardness and tensile strength.

The resistance to abrasive wear for the steel grade R260 after hot rolling and isothermal annealing is a function of the microstructure characteristics and steel properties, and of the operating conditions. The degree of wear depends strictly on the morphology of pearlite, which has a decisive influence on the properties of steel. The highest wear rate was observed for the steel after hot rolling. The structures after isothermal annealing proved to have higher resistance to abrasive wear. The smaller the interlamellar distance in cementite, the higher resistance to abrasive wear.

During the rail-vehicle riding through a turnout, a dynamic load is present as a result of the lack of continuity of the stretch of rails in the place of rails intersection. The values of load coming from rail vehicle wheels on the rolling surface of the rail sections depend on the mass and speed of the rail vehicle. Load imposed on a rail induces in the material, in the contact place, a particulate state of contact stresses. In specific cases, these values can be higher than the yield point value or the tensile strength of the material, which, as a result, may lead to subsurface cracks. The contract and reduced stress values determined in the numerical calculations depend on the load values. The highest reduced stresses occur in the contact zone and right under the rolling surface of the block section. The zone of action of stresses grows as the load increases.

References

[1] K. Aniołek, J. Herian, The structure, properties and a resistance to abrasive wear of railway sections of steel with a different pearlite morphology, IOP Conf. Series, Materials Science and Engineering 22 (2011) 012012.

[2] J. Herian, K. Aniołek, The structure and properties of steel with different pearlite morphology and its resistance to abrasive wear, Archives of Materials Science and Engineering 31/2 (2008) 83-86.

[3] G. Donzella, M. Faccoli, A. Ghidini, A. Mazzu, R. Roberti, The competitive role of wear and RCF in a rail steel, Engineering Fracture Mechanics 72 (2005) 287-308.

[4] L. Deters, M. Proksch, Friction and wear testing of rail and wheel material, Wear 258 (2005) 981-991.

[5] Z. Stradomski, S. Stachura, Role of microstructure in the mechanism of abrasive wear of high-carbon cast steels, Acta Metallurgica Slovaca R.8 2/2/2 (2002) 388-393.

[6] O.P. Modi, D.P. Mondal, B.K. Prasad, M. Singh, H.K. Khaira, Abrasive wear behaviour of a high carbon steel: effects of microstructure and experimental parameters and correlation with mechanical properties, Materials Science and Engineering A 343 (2003) 235-242.

[7] M.G.M. da F. Gomes, L.H. de Almeida, L.C.F.C. Gomes, I. Le May, Effects of microstructural parameters on the mechanical properties of eutectoid rail steels, Materials Characterization 39 (1997) 1-14.

[8] F.G. Caballero, C. Capdevila, C.G. de Andres, Modeling of the interlamellar spacing of isothermally formed pearlite in a eutectoid steel, Scripta Materialia 42 (2000) 537-542.

[9] F.G. Caballero, C.G. de Andres, C. Capdevila, Characterization and morphological analysis of pearlite in a eutectoid steel, Materials Characterization 45 (2000) 111-116.

[10] V.T.L. Buono, B.M. Gonzalez, T.M. Lima, M.S. Andrade, Measurement of fine pearlite interlamellar spacing by atomic force microscopy, Journal of Materials Science 32 (1997) 1005-1008.

[11] R. Kuziak, M. Głowacki, M. Pietrzyk, Modelling of plastic flow, heat transfer and microstructural evolution during rolling of eutectoid steel rods, Journal of Materials Processing Technology 60 (1996) 589-596.

[12] S. Zakharov, I. Zharov, Simulation of mutual wheel/rail wear, Wear 253 (2002) 100-106.

[13] V.M. Schastlivtsev, T.I. Tabatchikova, A.V. Makarov, L.Yu. Egorova, I.L. Yakovleva, Wear resistance of carbon steel with a structure of thin-plate pearlite, Metal Science and Heat Treatment 43/1-2 (2001) 30-33.

[14] D. Pogorelov, Computer-aided modeling railroad vehicle dynamics, Proceedings of the International Congress "Mechanics and Tribology of Transport Systems" Mechtribotrans 2003, Rostov on-Don, Book 2, 171-176.

[15] D.Y. Pogorelov, Simulation of rail vehicle dynamics with universal mechanism software, Rail vehicle dynamics and associated problems, Silesian University of Technology, Gliwice, 2005, 13-58.

[16] M. Polok-Rubiniec, L.A. Dobrzański, M. Adamiak, Comparison of the adhesion and wear resistance of the PVD coatings, Journal of Achievements in Materials and Manufacturing Engineering 20 (2007) 279-282.

[17] L.A. Dobrzański, D. Pakuła, Structure and properties of the wear resistant coatings obtained in the PVD and CVD processes on tool ceramics, Materials Engineering 3 (2004) 568-571.

[18] M. Sitarz, A. Sładkowski, Z. Żurek, Research of influence of surface profiles for different wheel - rail pair on distribution of contact stresses, Proceedings of the 6th International Conference "Contact mechanics and Wear of Rail/Wheel Systems" CHARMEC, Gothenburg, 2003, 259-264.

[19] M. Sitarz, T. Wojdyła, M. Witaszek, The forces and contact stresses in wheel - rail system, Proceedings of the International Conference "Mechanika", Kowno, 1999, 230-235.